
Discovering the Representation Bottleneck of Graph Neural Networks from Multi-order Interactions

Fang Wu*
Columbia University
New York, USA
fw2359@columbia.edu

Siyuan Li*
Westlake University
Hangzhou, China
lisiyuan@westlake.edu.cn

Lirong Wu
Westlake University
Hangzhou, China
wulirong@westlake.edu.cn

Dragomir Radev
Yale University
New Haven, CT, USA
dragomir.radev@yale.edu

Qiang Zhang
Zhejiang University
Hangzhou, China
qiang.zhang.cs@zju.edu.cn

Stan Z. Li†
Westlake University
Hangzhou, China
stan.zq.li@westlake.edu.cn

Abstract

Most graph neural networks (GNNs) rely on the message passing paradigm to propagate node features and build interactions. Recent works point out that different graph learning tasks require different ranges of interactions between nodes. To investigate the underlying mechanism, we explore the capacity of GNNs to capture pairwise interactions between nodes under contexts with different complexities, especially for their graph-level and node-level applications in scientific domains like biochemistry and physics. When formulating pairwise interactions, we study two standard graph construction methods in scientific domains, i.e., *K-nearest neighbor* (KNN) graphs and *fully-connected* (FC) graphs. Furthermore, we demonstrate that the inductive bias introduced by KNN-graphs and FC-graphs inhibits GNNs from learning the most informative order of interactions. Such a phenomenon is broadly shared by several GNNs for different graph learning tasks and prevents GNNs from reaching the global minimum loss, so we name it a *representation bottleneck*. To overcome that, we propose a novel graph rewiring approach based on the pairwise interaction strengths to adjust the reception fields of each node dynamically. Extensive experiments in molecular property prediction and dynamic system forecast prove the superiority of our method over state-of-the-art GNN baselines. Besides, this paper provides a reasonable explanation of why subgraphs play a vital role in determining graph properties. The code is available at <https://github.com/smiles724/bottleneck>.

1 Introduction

Over the past few years, *graph neural networks* (GNNs) [30, 72, 10, 44, 32, 20] have witnessed sharply growing popularity thanks to their ability to deal with broad classes of graphs with complex

*Equal contributions.

†The corresponding author.

relationships and interdependence between objects, ranging from social networks [21] to computer programs [59]. Particularly, GNNs show promising potential in scientific research. They are used to derive insights from structures of molecules [94] and reason about relations in a group of interacting objects [37]. For instance, chemists employ GNNs to reduce computation time for predicting molecular properties [73, 74, 95, 13, 96, 65, 101], where the complex interactions between atoms are modeled by passing messages. Many subsequent efforts have been devoted to fully leveraging 3D geometric information such as directions [48, 47] and dihedral angles [45, 54]. Physicists also utilize GNNs to characterize arbitrarily ordered objects and combinatorial relations. Some employ Interaction Networks [5] to model particle systems in diverse physical domains [52, 58, 68]. Since physical rules stay stable regardless of the reference coordinate system, several works [39, 27, 38, 70] have explored equivariance upon GNNs and showed remarkable benefits.

As a consequence, the startling success of GNNs provokes the bottleneck question—“Are there any common limitations of GNNs in real-world modeling applications, such as molecules and dynamic systems?” Knowing that GNNs are typically expressed as a neighborhood aggregation or message passing scheme [29, 84], we leverage the interactions between input variables [18] to investigate the bottleneck of GNNs in graph learning. That is, we aim to analyze which types of interaction patterns (e.g., certain physical or chemical concepts) are likely to be encoded by GNNs, and which other types are difficult to manipulate.

As a relevant answer to the bottleneck question mentioned above, the preceding work observes the liability of CNNs to capture too complex and too simple interactions [18], which differs dramatically from human recognition. To comprehensively explore the representation capability of GNNs, we refine the measurement of multi-order pairwise interactions so that the metric works for both node-level and graph-level predictions. When formulating the pairwise interactions, we study two common graph construction methods in scientific domains, including *K-nearest neighbor* (KNN) graphs and *fully-connected* (FC) graphs. Then with massive empirical evidence from two real-world graph learning problems—molecular representation learning and dynamic system modeling, we discover that, as opposed to CNNs’ behavior, GNNs are astonishingly more capable of encoding intermediate complexity interactions. This discovery is perfectly consistent with the practice that pharmacologists are interested in identifying subgraphs that primarily represent specific molecular properties, e.g., functional groups [29, 40, 99, 86].

Despite that inclination, we detect that the imperfect inductive bias introduced by KNN-graphs and FC-graphs prohibits GNNs from encoding a particular order of interactions, so they fail to achieve the global minimum loss. We name this phenomenon as *a representation bottleneck* of GNNs. To resolve this obstacle, we propose a novel graph rewiring technique based on the distribution of interaction strengths, which progressively optimizes the inductive bias of GNNs via calibrating the topological structures of input graphs. Experiments on both synthetic and real-world datasets validate the superiority of our method in terms of GNN interpretability and generalization.

2 Preliminary

Multi-order interactions. Suppose a graph has a set of N variables of interest (a.k.a. nodes). It could represent a macroscopic physical system with N celestial bodies, or a microscopic biochemical system with N atoms or particles, denoted as $[N]$. Given a pre-trained GNN model f , let $f([N])$ represent the model output of all input variables. For node-level tasks, the GNN forecasts a value (e.g., atomic energy) or a vector (e.g., atomic force or velocity) for each node. For graph-level predictions, $f([N]) \in \mathbb{R}$ is a scalar (e.g., drug toxicity or binding affinity) for classification and regression. GNNs make predictions by interactions between input variables instead of working individually on each variable [63, 53, 56, 36]. Previous studies [7, 81, 100, 18] mainly concentrate on the pairwise interactions and use the multi-order interaction $I^m(i, j)$ to measure interactions of different complexities between two input variables $i, j \in [N]$.

Representation bottleneck. Specifically, the m -th order interaction $I^{(m)}(i, j)$ measures the average interaction utility between variables i, j under all possible contexts consisting of m variables. Mathematically, the multi-order interaction is defined as follows:

$$I^{(m)}(i, j) = \mathbb{E}_{S \subseteq [N], \{i, j\} \subseteq S, |S|=m} [\Delta f(i, j, S)], 3 \leq m \leq N, \quad (1)$$

where $\Delta f(i, j, S) = f(S) - f(S \setminus \{i\}) - f(S \setminus \{j\}) + f(S \setminus \{i, j\})$ and $S \in [N]$ is the context consisting of m variables. $f(S)$ is the output when we keep variables in S unchanged but alter variables in $[N] \setminus S$. Since it is irrational to feed an empty graph into a GNN, we demand the context S to have at least one variable with $m \geq 3$ and omit the $f(\emptyset)$ term. Note that Zhang et al. [100] assume variables i, j do not belong to the context S . Contrarily, we argue that it is more reasonable to interpret m as the contextual complexity of the interaction if variables i, j are included in the context, and provide a proof in Appendix A.1 that these two cases are equivalent but from different views.

To measure the reasoning complexity of the DNN, researchers compute the relative interaction strength $J^{(m)}$ of the encoded m -th order interaction as follows:

$$J^{(m)} = \frac{\mathbb{E}_{x \in \Omega} [\mathbb{E}_{i, j} [|I^{(m)}(i, j | x)|]]}{\sum_{m'} \mathbb{E}_{x \in \Omega} [\mathbb{E}_{i, j} [|I^{(m')}(i, j | x)|]]}, \quad (2)$$

where Ω stands for the set of all samples, and the strength $J^{(m)}$ is calculated over all pairs of input variables in all data points. Then normalize $J^{(m)}$ by the summation value of $I^{(m)}(i, j | x)$ with different orders rather than the average value in [18] to constrain $0 \leq J^{(m)} \leq 1$ for explicit comparison across various tasks and datasets.

According to the efficiency property of $I^{(m)}(i, j)$ [18], the change of DNN parameters ΔW can be decomposed as the sum of gradients $\frac{\partial I^{(m)}(i, j)}{\partial W}$. Mathematically, we denote L as the loss function and η as the learning rate. With $U = \sum_{i \in N} f(\{i\})$, and $R^{(m)} = -\eta \frac{\partial L}{\partial f(N)} \frac{\partial f(N)}{\partial I^{(m)}(i, j)}$, it can be attained:

$$\Delta W = -\eta \frac{\partial L}{\partial W} = -\eta \frac{\partial L}{\partial f(N)} \frac{\partial f(N)}{\partial W} = \Delta W_U + \sum_{m=3}^n \sum_{i, j \in N, i \neq j} R^{(m)} \frac{\partial I^{(m)}(i, j)}{\partial W}, \quad (3)$$

3 Revisiting Bottlenecks of DNNs

Before investigating the representation bottleneck of GNNs, we first retrospect relevant findings of DNNs. With this Equ. 3, Deng et al. [18] use $\Delta W^{(m)}(i, j) = R^{(m)} \frac{\partial I^{(m)}(i, j)}{\partial W}$ to represent the compositional component of ΔW w.r.t. $\frac{\partial I^{(m)}(i, j)}{\partial W}$ and claim that it is proportional to $F^{(m)} = \frac{n-m+1}{n(n-1)} / \sqrt{\binom{n-2}{m-2}}$. Despite their delicate theoretical framework, a simple counterexample is when $\frac{m}{n} \rightarrow 0$ or $\frac{m}{n} \rightarrow 1$, $F^{(m)}$ ought to be approximately the same (see Fig. 1). This is in conflict with the experimental curves in [18], where $J^{(m)}$ of low-order (e.g., $m = 0.05n$) is much higher than that of high-order (e.g., $m = 0.95n$).

Notably, there we disregard the empty set \emptyset as the input for DNNs. In Appendix A.2, we demonstrate that even if $f(\emptyset)$ is taken into consideration, once n is large (e.g., $n \geq 100$), $J^{(m)}$ ought to be non-zero only when $\frac{m}{n} \rightarrow 0$. This phenomenon indicates that DNNs fail to capture any middle-order or high-order interactions, which is strongly opposed to the truth that DNNs perform well in tasks that require high-order interactions such as protein interface prediction [55].

Based on this fact, we ascribe Deng et al. [18]'s inaccurate statement to their flawed assumption. To be explicit, we show empirically in Appendix C.3, where the hypothesis that the derivatives of $\Delta f(i, j, S)$ over model parameters, i.e., $\frac{\partial \Delta f(i, j, S)}{\partial W}$, conform to normal distributions should be rejected. On the contrary, $\frac{\partial \Delta f(i, j, S)}{\partial W}$ varies along with the contextual complexities (i.e., $|S|$), which is heavily dependent on the data distribution of interaction strengths in particular datasets as well as the chosen model

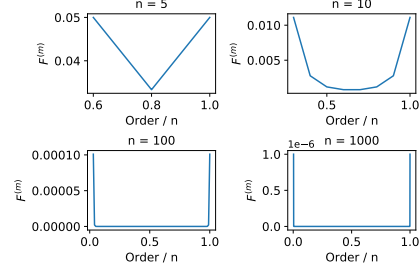


Figure 1: The theoretical distributions of $F^{(m)}$ under different n .

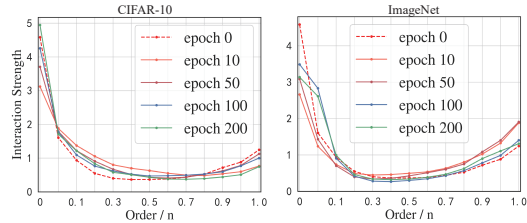


Figure 2: The change of interaction strengths for ResNet on CIFAR-10 and ImageNet, measured after various training epochs.

architectures f . $\frac{\partial \Delta f(i,j,S)}{\partial W}$ contains information within crucial orders of interactions that data drives the model to focus on through backpropagation. There, we define the data distribution of interaction strengths on the dataset D , denoted as $J_D^{(m)}$, as the experimental distribution of interaction strengths for some model f with randomly initialized parameters. Accordingly, the learned interaction strength $J^{(m)}$ should be attributed more to $J_D^{(m)}$, which discloses the most informative orders of interactions to realize lower errors in specific tasks, rather than to a spurious proportion value $F^{(m)}$.

To further support our conjecture, we re-produce experiments in [18]. Fig. 2 implies that $J_D^{(m)}$ (referring to the epoch-0 curve) in image datasets including CIFAR-10 [49] and ImageNet [67], coincidentally follow a pattern that low-order and high-order interactions are much stronger than middle-order, and little difference exists between $J_D^{(m)}$ and $J^{(m)}$ (referring to those non-zero epoch curves) at different epochs. Thus, the change of $J^{(m)}$ during the training process cannot verify the tendency or bottleneck that DNNs would concentrate more on low-order and high-order but neglect middle-order interactions. In contrast, our subsequent experiments have confirmed the fact that GNNs are more inclined to emphasize interactions of middle-level complexities.

4 Representation Bottleneck of GNNs

4.1 Node-level Multi-order Interaction

$I^{(m)}(i,j)$ in Equ. 1 is designed to analyze the influence of interactions over the integral system (e.g., a molecule or a galaxy) and is therefore only suitable in the circumstance of graph-level prediction. No such metric exists to measure the effects of those interactions on each component (e.g., atom or particle) of the system. To overcome this limitation, we propose a new metric as the following:

$$I_i^{(m)}(j) = \mathbb{E}_{S \subseteq [N], \{i,j\} \subseteq S, |S|=m} [\Delta f_i(j, S)], 2 \leq m \leq N, \quad (4)$$

where $\Delta f_i(j, S) = \|f_i(S) - f_i(S \setminus \{j\})\|_p$, and $\|\cdot\|_p$ is the p -norm if $f_i(\cdot)$ outputs a vector instead of a scalar. We denote $f_i(S)$ as the output for the i -th variable when variables in S is kept unchanged. Then the corresponding node-level interaction strength is defined as $J^{(m)} = \frac{\mathbb{E}_{x \in \Omega} [\mathbb{E}_i [\mathbb{E}_j [\mathbb{E}_x [I_i^{(m)}(j|x)]]]]}{\sum_{m'} \mathbb{E}_{x \in \Omega} [\mathbb{E}_i [\mathbb{E}_j [\mathbb{E}_x [I_i^{(m')} (j|x)]]]]}$. This novel metric in Equ. 4 allows us to measure the representation capability of GNNs in node-level classification or regression tasks.

4.2 Graph Constructions for Scientific Problems

KNN vs. fully-connected graphs. How to handle variables in $[N] \setminus S$ is critical to the formulation of $I^{(m)}(i,j)$. Nonetheless, the widely-used setting in Ancona et al. [2] for sequences or pixels is not applicable there. Contrarily, in real-world scenarios, including molecules or dynamic systems, the most crucial feature of variables (atoms or particles) is their classes (e.g., one-hot embeddings). A simple average over different molecules or systems can lead to the ambiguous atom or particle types. As an alternative, we consider dropping these variables in $[N] \setminus S$ instead of replacing them with a mean value. In particular, the deletion of those variables ought to satisfy the two succeeding properties: (1) The resulting subgraph must maintain the connectivity, where entities can reach others freely. Otherwise, if it generates multiple disjoint subgraphs, each subgraph would be an entirely independent system. This breaks the fundamental assumption in nature that molecules or dynamic systems are an organic whole and indivisible. (2) No ambiguity is intrigued from both the structural view and feature view. For instance, an element with an invalid atomic number of 3.64 is not permitted.

To achieve these two properties, we employ the K-nearest-neighbor (KNN) algorithm to construct graphs based on pairwise distances in the 3D space (named KNN-graph, see Fig. 3 (a)), a common technique for building edges in macromolecules [24, 28, 77]. When we desire to centre on S and ignore other variables, subgraphs are re-constructed via KNN to

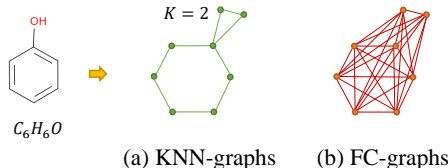


Figure 3: Different graph constructions of the compound C_6H_6O .

ensure connectivity. We also act our analysis on fully-connected graphs (named FC-graph, see Fig. 3 (b)), where all atoms or particles are connected to each other [12, 91, 3, 41]. Consequently, removing any entity in FC-graphs will not influence the association of other pairs. In fact, FC-graphs are a special type of KNN-graphs, where $K \geq N - 1$.

Notably, unlike social networks or knowledge graphs, edges in scientific graphs are usually not explicitly defined. KNN-graphs and FC-graphs are broad practices to establish connections between entities. However, FC-graphs or KNN-graphs with a large K suffer from high computational expenditure and are usually infeasible with thousands of entities. In addition, they are sometimes unnecessary since the impact from distant nodes is so minute to be ignored.

4.3 Graph Rewiring for Inductive Bias Optimization

The bottleneck of GNNs. While the former analysis on images indicates that $J_D^{(m)}$ of CNNs dominantly decides $J^{(m)}$, our experiments on graphs (see Section 5.2) exhibit $J^{(m)}$ of GNNs deviates from $J_D^{(m)}$. This motivates us to investigate what truly determines $J^{(m)}$.

Concerning CNNs, the locality is one critical inductive bias. It assumes that entities are in spatially close proximity with one another and isolated from distant ones [6], hence CNNs are bound to low-order interactions. To farther testify our argument, we examine the change of interaction strengths for MLP using MLP-Mixer [79] in Fig. 4. Though MLP shares a similar $J_D^{(m)}$ with CNN but its $J^{(m)}$ is much smoother. This is because MLP-Mixer is not constrained by the inductive bias of locality and can learn a more adorable $J^{(m)}$. Indeed, since graphs support arbitrary pairwise relational structures [6], the inductive bias of GNNs is more flexible. It primarily depends on how to establish the topology of graphs and heavily influences $J^{(m)}$. For example, FC-graphs consist of all pairwise relations, while in KNN-graphs, some pairs of entities possess a relation and others do not. These graph construction mechanisms can bring improper inductive bias, resulting in a poor $J^{(m)}$ and becoming the representation bottleneck of GNNs.

Accordingly, a more intriguing question would be what is the optimal inductive bias. In this work, we rely on the most informative order m^* of interactions to modify the inductive bias of GNNs. Consequently, models are regulated to be apt to interactions of a certain order, and $J^{(m)}$ are also adjusted. For modern GNNs, the loss L is typically non-convex with multiple local and even global minima [22] that may yield similar values of L while acquiring significantly different capacities to learn interactions (i.e., significantly different $J^{(m)}$). As declared in Prop. 1 (the explanation is in Appendix A.3), if $J^{(m)}$ is not equivalent to the optimal strength $J^{(m)*}$, then the corresponding model f must be stuck in a local minimum point of the loss surface. Recent work [18] imposes two losses to encourage or penalize the learning of interactions of specific complexities. Nevertheless, they require models to make accurate predictions on subgraphs, but variable removal brings the out-of-distribution (OOD) problem [11, 26, 87]. Such OOD subgraphs can manipulate GNNs’ outcome arbitrarily and produce erroneous predictions [16, 102]. More importantly, these losses are based on the assumption that the image class remains regardless of pixel removal. However, it is not rational to assume that the properties of molecules or dynamic systems will be stable if we alter their components. Thus, instead of intervening the loss, we attempt to alter the inductive bias of GNNs for the sake of learning $J^{(m)*}$.

Proposition 1 *Let $J^{(m)*}$ be the interaction strength of the function f^* that achieves the global minimum loss L^* in data D . If another model f' converges to a loss L' after the parameters update and $J^{(m)'} \neq J^{(m)*}$, then L' must be a local minimum loss, i.e. $L' > L^*$.*

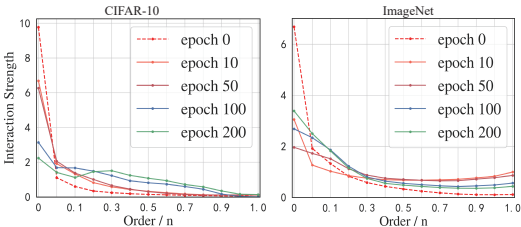


Figure 4: The change of interaction strengths for MLP-Mixer on CIFAR-10 and ImageNet.

Graph rewiring. Unfortunately, $J^{(m)*}$ can never be known unless sufficient domain knowledge is supplied. However, we can observe from Fig. 2 that in the initial training epochs (e.g., 10 or 50 epochs), CNNs do not directly dive into low-order of interactions. Instead, they still have the inclination to deviate from $J_D^{(m)}$ and learn more informative order of interactions (e.g., middle-order) regardless of the inductive bias. Motivated by this subtle tendency, we resort to the order of interactions that increase the most during training in $J^{(m)}$ as the guidance to reconstruct graphs and estimate $J^{(m)*}$. To this end, we dynamically adjust the reception fields of each entity within molecules or systems by establishing or destroying edges, as described in Algorithm 1. Such a method is often generically referred to as *graph rewiring* [80]. By adjusting graph topology, i.e., the inductive bias of GNNs, the bottleneck of GNNs is broken, and $J^{(m)}$ is able to gradually approximate $J^{(m)*}$. Simultaneously, the training loss can finally reach the global minimum after gradient descent (see Fig. 5). Emphatically, our algorithm (named ISGR) is applicable for both KNN-graphs and FC-graphs, though the latter starts with an adequately large $k_0 \geq N - 1$.

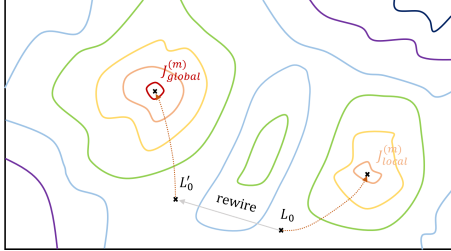


Figure 5: Transformation of the training loss with graph rewiring in the loss surface.

Algorithm 1 Interaction Strength-based Graph Rewiring (ISGR) Algorithm.

Require: nodes V , pairwise distance d , number of neighbors k_0 , threshold \bar{J} , epoch interval Δe
Construct a KNN-graph with $K = k_0$ based on d and compute the initial interaction strength $J_0^{(m)}$;
for each Δe epochs **do**
 Sample a mini-batch B and calculate the corresponding interaction strengths $J_B^{(m)}$;
 if the maximum increase of some order exceeds \bar{J} , i.e., $\max(\Delta J^{(m)}) \geq \bar{J}$ **then**
 Find the order whose interaction strength increases the most $m^* = \underset{m}{\operatorname{argmax}}(\Delta J^{(m)})$;
 Increase the number of neighboring nodes k if $m^* > k$, otherwise decrease k ;
 Reconstruct a KNN-graph with $K = k$ and train the model with this new graph structure.
 end if
end for

5 Experimental Settings and Results

In this section, we present four case studies where the aforementioned framework is applied to analyze the representation bottleneck problem of GNNs for scientific research. Among them, Newtonian dynamics and molecular dynamics simulations are node-level prediction tasks, while Hamiltonian dynamics and molecular property prediction are graph-level prediction tasks. More experimental details are elucidated in Appendix C.

5.1 Data and Set Up

Newtonian dynamics. Newtonian dynamics [89] describes the dynamics of particles according to Newton’s law of motion: the motion of each particle is modeled using incident forces from nearby particles, which changes its position, velocity, and acceleration. Several important forces in physics, such as the gravitational force, are defined on pairs of particles, analogous to the message function of GNNs [15]. We adopt the N-body particle simulation dataset in [15]. It consists of N-body particles under six different interaction laws. More details can be referred to Appendix C.1.

Hamiltonian dynamics. Hamiltonian dynamics [31] describes a system’s total energy $\mathcal{H}(\mathbf{q}, \mathbf{p})$ as a function of its canonical coordinates \mathbf{q} and momenta \mathbf{p} , e.g., each particles’ position and momentum. The dynamics of the system change perpendicularly to the gradient of \mathcal{H} : $\frac{d\mathbf{q}}{dt} = \frac{\partial \mathcal{H}}{\partial \mathbf{p}}$, $\frac{d\mathbf{p}}{dt} = -\frac{d\mathcal{H}}{d\mathbf{q}}$. There we take advantage of the same datasets from Newtonian dynamics case study, and attempt to learn the scalar total energy \mathcal{H} of the system.

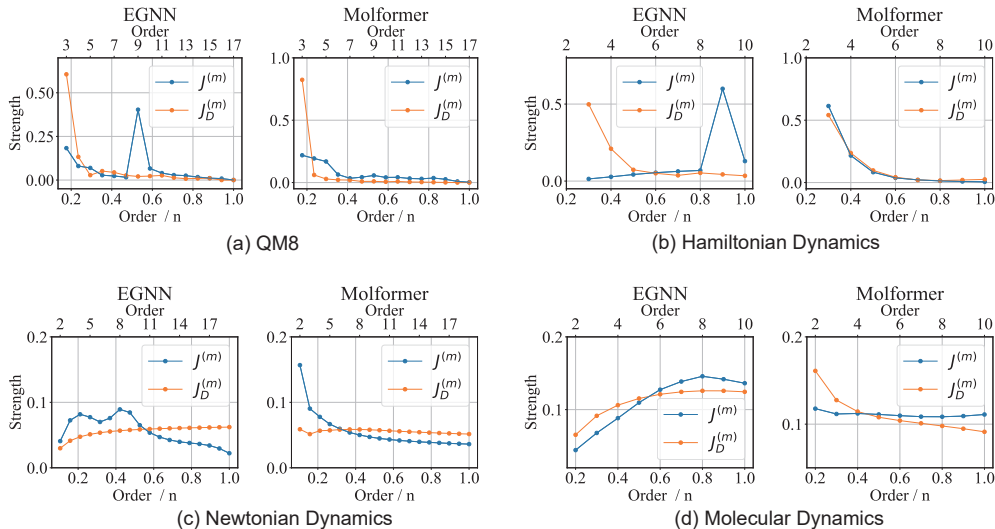


Figure 6: Distributions of interaction strengths of EGNN and Molformer in graph-level and node-level prediction tasks. We use double-x axes to represent the order m and the ratio $\frac{m}{n}$.

Molecular dynamics simulations. Molecular dynamics (MD) [25, 42, 82] has long been the *de facto* choice for modeling complex atomistic systems from first principles. There MD simulations are carried out using the standard quantum chemistry computational method, density functional theory (DFT), which is different from the classic force field in Newtonian dynamics.

There we adopt the ISO17 dataset [73, 74], which is generated from MD simulations using the Fritz-Haber Institute *ab initio* simulation package [9]. ISO17 consists of 129 molecules, each containing 5K conformational geometries and total energies with a resolution of 1 femtosecond in the trajectories. Our target is to predict the atomic forces of the molecule at different timeframes.

Molecular property prediction. The forecast of a broad range of molecular properties is a fundamental task in the field of drug discovery [19]. The acceleration of finding better drug candidates is compelling since the average cost for a new drug is at a sky-high price [98], where DL methods, especially GNNs, play an irreplaceable role [90]. The properties in current molecular collections can be mainly divided into four categories: quantum mechanics, physical chemistry, biophysics, and physiology, ranging from molecular-level properties to macroscopic influences on the human body [94].

We utilize two benchmark datasets. QM7 [8] is a subset of GDB-13 and is composed of 7K molecules. QM8 [64] is a subset of GDB-17 with 22K molecules. Note that QM7 and QM8 provide one and twelve properties, respectively, and we merely use the *E1-CC2* property in QM8 for simplicity.

Backbones. In our experiments, two state-of-the-art geometric GNNs are selected to perform on these two graph types. We pick up *equivariant graph neural network* (EGNN) [70] for KNN-graphs, and *Molformer* [91] with no motifs for FC-graphs. EGNN is roto-translation and reflection equivariant without the spherical harmonics [78]. Molformer is a variant of Transformer [83, 34], designed for molecular graph learning.

5.2 Results and Visualization.

The learned distribution of interaction strengths can deviate from the data distribution.

Fig. 6 reports the learned distributions $J^{(m)}$ and the data distributions $J_D^{(m)}$ for both graph-level and node-level tasks. The complementary plots for QM7 are available in Appendix C.4. From these curves, we can draw firmly that unlike CNNs in Fig. 2, $J^{(m)}$ of GNNs can be divergent from $J_D^{(m)}$.

For molecular property prediction, $J_D^{(m)}$ is more intensive on low-order ($\frac{m}{n} \leq 0.3$). But after sufficient training, $J^{(m)}$ for EGNN mainly have high values for middle-order interactions ($0.5 \leq \frac{m}{n} \leq 0.8$), and the middle-order segment ($0.4 \leq \frac{m}{n} \leq 0.6$) of $J^{(m)}$ for Molformer also increases the most.

This illustrates that subgraphs with a middle size are the very informative substructures to reveal the biological or chemical properties of small molecules. This finding persistently accords with the fact that motifs such as functional groups play a key part in determining molecular attributes [99, 86, 92]. While for Hamiltonian dynamic systems, $J_D^{(m)}$ is majorly intense for low-order and middle-order interactions ($\frac{m}{n} \leq 0.6$). In spite of that, $J^{(m)}$ of EGNN concentrates more on high-order ($0.7 \leq \frac{m}{n} \leq 0.9$) but neglect low-order ($\frac{m}{n} \leq 0.5$).

Regarding node-level prediction tasks, the scenery is more straightforward. Though $J^{(m)}$ for EGNN and Molformer are in different shapes, they both moves towards low-order interactions ($\frac{m}{n} \leq 0.3$) for Newtonian dynamics and high-order interactions for MD ($\frac{m}{n} \geq 0.7$). All those phenomenons demonstrate considerable discrepancies between $J^{(m)}$ and $J_D^{(m)}$ for GNNs.

The inductive bias heavily determines the change of learned distributions. Unequivocally, the inclines of EGNN and Molformer to learn interactions of specific orders are distinct. Due to the inductive bias introduced by KNN-graphs, EGNN is more prone to pay attention to interactions of K th-order (e.g., $K = 8$ in our setting). Contrarily, Molformer, based on FC-graphs, assumes that all particles can affect each other directly, resulting in a more unconstrained $J^{(m)}$. For example, its $J^{(m)}$ on Newtonian dynamics is extremely smooth like a straight line, but its $J^{(m)}$ on Hamiltonian and MD are steep curves. All these evidences bolster our proposal that the inductive bias brought by the topological structure of input graphs has a significant impact on $J^{(m)}$ of GNNs.

Particularly, KNN-graphs are more susceptible to improper inductive bias, which prevents EGNN concerning interactions of orders that differ from K and can lead to worse performance. However, FC-graphs (or KNN-graphs with a large K) are not a panacea for all tasks. Except that FC-graphs require much more computational costs and may be prohibited for the case of tremendous entities, the performance of Molformer severely depends on the sufficiency and quality of training data. As shown in Tab. 2, Molformer does not surpass EGNN on all datasets. Instead, it behaves worse than EGNN on Hamiltonian ($1.250 > 0.892$) and MD ($0.736 > 0.713$), which motivates us to challenge the inductive bias of FC-graphs and resort to KNN-graphs occasionally.

5.3 Investigation of the GNN Bottleneck

Ablation studies. In Section 3.4, we propose an ISGR method to dynamically optimize the inductive bias of GNNs. There we conduct experiments to examine its efficiency, and results are reported with the mean and standard deviation of three repetitions in Tab. 1 and 2. It can be observed that our ISGR algorithm significantly improves the performance of EGNN and Molformer on all graph-level and node-level tasks. Particularly, the promotion for EGNN is much higher, which confirms our assertion that GNNs based on KNN-graphs are more likely to suffer from the bad inductive bias. On the other hand, the improvement for Molformer in QM7 is more considerable than QM8. This proves that GNNs based on FC-graphs are more easily affected by inappropriate inductive bias (i.e., full connection) when the data is insufficient, since the size of QM7 (7K) is far smaller than QM8 (21K).

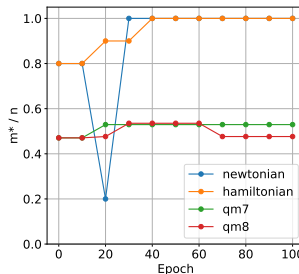


Figure 7: The change of m^* over epochs for EGNN.

The change of m^* during training. We plot the variation tendency of m^* over different epochs in Fig. 7. It shows that different tasks enjoy various optimal K (denoted as K^*). Explicitly, Hamiltonian dynamics and Newtonian dynamics benefit from full-connection ($\frac{K^*}{n} = 1$), while the molecular property prediction including QM7 and QM8 benefits more from middle-order interactions ($\frac{K^*}{n} \approx 0.5$). This phenomenon perfectly fits to the physical laws, because the system in Newtonian

Table 1: Comparison of performance with (w.) and without (w/o) the ISGR mechanism for node-level prediction tasks.

Model	Newtonian Dynamics		MD	
	EGNN	Molformer	EGNN	Molformer
w/o	6.951 \pm 0.098	1.929 \pm 0.051	1.409 \pm 0.082	0.848 \pm 0.053
w.	4.734 \pm 0.103	1.879 \pm 0.066	0.713 \pm 0.097	0.736 \pm 0.048

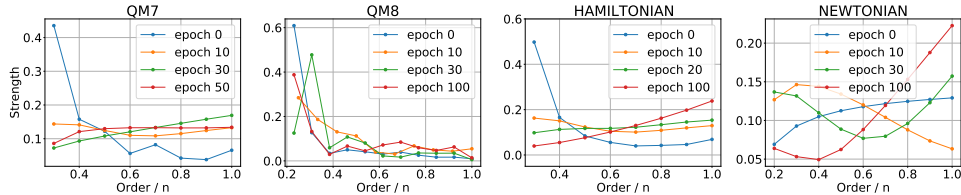


Figure 8: The change of interaction strengths with different training epochs for EGNN on different tasks.

and Hamiltonian datasets is extremely compact with close pairwise distances. Those particles are more likely to be influenced by all the other nodes.

The change of interaction strengths during training. Fig. 8 depicts how $J^{(m)}$ changes when the training proceeds with our ISGR algorithm. Although for data like QM7, QM8, and Hamiltonian dynamics, $J_D^{(m)}$ mostly concentrate on low-order interactions ($\frac{m}{n} \leq 0.4$), $J^{(m)}$ progressively adjust to middle-order and high-order ($\frac{m}{n} \geq 0.4$). Regarding Newtonian dynamics, $J_D^{(m)}$ is very smooth, but $J^{(m)}$ at initial epochs (i.e., 10 and 20 epochs) oddly focus on low-order interactions ($\frac{m}{n} \leq 0.4$). Nevertheless, our ISGR method timely corrects the wrong tendency and eventually, $J^{(m)}$ becomes more intensive in segments of middle-order and high-order ($\frac{m}{n} \geq 0.6$).

6 Related Work

The representation capacity of GNNs. It has become an emerging area to evaluate the representation capability of DNNs. Previous researches mainly study the theoretically maximum complexity [76], generalization ability [61, 88, 23], and robustness [60] of DNNs. Zhang et al. [100] and Deng et al. [18] are pioneers to focus on the limitation of DNNs in feature representations by means of variable interactions. Notwithstanding, these prior works highlight the behaviors of general DNNs and experimentally examine their assertions via MLP and CNNs. In comparison, we focus on GNNs that operate on structured graphs, which are very distinct from images and texts.

More relevantly, Barceló et al. [4] finds that the expressiveness of GNNs captures only a tiny fragment of first-order logic. This arises from the inability of a node to be aware of distant nodes that are farther away than the number of total layers. However, GNNs are observed not to benefit from the increase of layers due to the *over-smoothing* dilemma [51, 46, 14]. Recently, Alon and Yahav [1] proposes the existence of the *over-squashing* phenomenon for GNNs to grab long-range interactions and modify the last GNN layer to operate on a FC-graph. To take a step further, Topping et al. [80] proves that negatively curved edges are responsible for the *over-squashing* issue and introduces a curvature-based graph rewiring approach to alleviate that. More related works in regards to the representation capability of GNNs are in Appendix D. But none of them considers GNNs’ capacity in encoding pairwise interactions. To the best of our knowledge, we are among the first to understand of GNNs’ representation capability from the perspective of interactions under different contextual complexities and link it with their inductive bias. An interesting discussion regarding motif-based heterogeneous graphs from the view of our discovered bottleneck is in Appendix E.

Explainable GNNs for science. Variants of GNNs have shown ground-breaking performance in the field of natural science [5, 69, 68]. However, most GNNs are black boxes that are too complicated for scientists to comprehend and interpret the results [66]. Growing efforts have been made towards their explainability. For example, Cranmer et al. [15] perform symbolic regression to components of well-trained GNNs and extract compact closed-form analytical expressions. A more mainstream line is to recognize an informative yet compressed subgraph from the original graph [99, 86, 87, 92]. Identification of those subgraphs promotes GNNs to audit their inner workings and justify their predictions [92], which can shed light on meaningful scientific tasks like protein structure prediction [75]. Our work devises a contextual-aware method to comprehensively understand what complexity of interactions are the most influential and best interpret the decisions of GNNs.

Table 2: Comparison of performance with (w.) and without (w/o) the ISGR mechanism for graph-level prediction tasks.

Model	Hamiltonian Dynamics		QM7		QM8	
	EGNN	Molformer	EGNN	Molformer	EGNN	Molformer
w/o	1.392 ± 0.042	1.545 ± 0.036	68.182 ± 3.581	51.119 ± 2.193	0.012 ± 0.001	0.012 ± 0.001
w.	0.892 ± 0.051	1.250 ± 0.029	53.134 ± 2.711	34.439 ± 4.017	0.011 ± 0.000	0.010 ± 0.001

7 Conclusion

In this paper, we have discovered and strictly analyzed the representation bottleneck of GNNs from the view of the complexity of interactions encoded in networks. Remarkably, middle-order interactions are dominantly meaningful in the expressions of GNNs than low-order or high-order interactions. This offers a novel explanation to a well-known belief that subgraphs (e.g., motifs) contribute to recognizing graph properties.

Apart from that, we distinguish the robust relatedness between the inductive bias of GNNs and their learned distribution of interaction strengths. This observation concludes that inductive biases introduced by most graph construction mechanisms such as KNN and full connection can be sub-optimal. Inspired by this gap, we design a novel graph rewiring method to optimize the inductive bias based on the inclination of GNNs to encode more informative orders of interactions. We conduct a broad range of experiments on four synthetic and real-world tasks, and the results verify that GNNs are allowed to reach the global minimum loss and break the bottleneck via our efficient algorithm.

References

- [1] Alon, U., Yahav, E., 2020. On the bottleneck of graph neural networks and its practical implications. arXiv preprint arXiv:2006.05205 .
- [2] Ancona, M., Oztireli, C., Gross, M., 2019. Explaining deep neural networks with a polynomial time algorithm for shapley value approximation, in: International Conference on Machine Learning, PMLR. pp. 272–281.
- [3] Baek, M., DiMaio, F., Anishchenko, I., Dauparas, J., Ovchinnikov, S., Lee, G.R., Wang, J., Cong, Q., Kinch, L.N., Schaeffer, R.D., et al., 2021. Accurate prediction of protein structures and interactions using a three-track neural network. *Science* 373, 871–876.
- [4] Barceló, P., Kostylev, E., Monet, M., Pérez, J., Reutter, J., Silva, J.P., 2020. The logical expressiveness of graph neural networks, in: 8th International Conference on Learning Representations (ICLR 2020).
- [5] Battaglia, P., Pascanu, R., Lai, M., Jimenez Rezende, D., et al., 2016. Interaction networks for learning about objects, relations and physics. *Advances in neural information processing systems* 29.
- [6] Battaglia, P.W., Hamrick, J.B., Bapst, V., Sanchez-Gonzalez, A., Zambaldi, V., Malinowski, M., Tacchetti, A., Raposo, D., Santoro, A., Faulkner, R., et al., 2018. Relational inductive biases, deep learning, and graph networks. arXiv preprint arXiv:1806.01261 .
- [7] Bien, J., Taylor, J., Tibshirani, R., 2013. A lasso for hierarchical interactions. *Annals of statistics* 41, 1111.
- [8] Blum, L.C., Raymond, J.L., 2009. 970 million druglike small molecules for virtual screening in the chemical universe database gdb-13. *Journal of the American Chemical Society* 131, 8732–8733.
- [9] Blum, V., Gehrke, R., Hanke, F., Havu, P., Havu, V., Ren, X., Reuter, K., Scheffler, M., 2009. Ab initio molecular simulations with numeric atom-centered orbitals. *Computer Physics Communications* 180, 2175–2196.
- [10] Bruna, J., Zaremba, W., Szlam, A., LeCun, Y., 2013. Spectral networks and locally connected networks on graphs. arXiv preprint arXiv:1312.6203 .
- [11] Chang, C.H., Creager, E., Goldenberg, A., Duvenaud, D., 2018. Explaining image classifiers by counterfactual generation. arXiv preprint arXiv:1807.08024 .
- [12] Chen, B., Barzilay, R., Jaakkola, T., 2019a. Path-augmented graph transformer network. arXiv preprint arXiv:1905.12712 .
- [13] Chen, C., Ye, W., Zuo, Y., Zheng, C., Ong, S.P., 2019b. Graph networks as a universal machine learning framework for molecules and crystals. *Chemistry of Materials* 31, 3564–3572.
- [14] Chen, D., Lin, Y., Li, W., Li, P., Zhou, J., Sun, X., 2020. Measuring and relieving the over-smoothing problem for graph neural networks from the topological view, in: Proceedings of the AAAI Conference on Artificial Intelligence, pp. 3438–3445.
- [15] Cranmer, M., Sanchez Gonzalez, A., Battaglia, P., Xu, R., Cranmer, K., Spergel, D., Ho, S., 2020. Discovering symbolic models from deep learning with inductive biases. *Advances in Neural Information Processing Systems* 33, 17429–17442.
- [16] Dai, H., Li, H., Tian, T., Huang, X., Wang, L., Zhu, J., Song, L., 2018. Adversarial attack on graph structured data, in: International conference on machine learning, PMLR. pp. 1115–1124.
- [17] Das, S., Chakrabarti, S., 2021. Classification and prediction of protein–protein interaction interface using machine learning algorithm. *Scientific reports* 11, 1–12.
- [18] Deng, H., Ren, Q., Chen, X., Zhang, H., Ren, J., Zhang, Q., 2021. Discovering and explaining the representation bottleneck of dnns. arXiv preprint arXiv:2111.06236 .

- [19] Drews, J., 2000. Drug discovery: a historical perspective. *science* 287, 1960–1964.
- [20] Dwivedi, V.P., Joshi, C.K., Laurent, T., Bengio, Y., Bresson, X., 2020. Benchmarking graph neural networks. *arXiv preprint arXiv:2003.00982* .
- [21] Fan, W., Ma, Y., Li, Q., He, Y., Zhao, E., Tang, J., Yin, D., 2019. Graph neural networks for social recommendation, in: *The world wide web conference*, pp. 417–426.
- [22] Foret, P., Kleiner, A., Mobahi, H., Neyshabur, B., 2020. Sharpness-aware minimization for efficiently improving generalization. *arXiv preprint arXiv:2010.01412* .
- [23] Fort, S., Nowak, P.K., Jastrzebski, S., Narayanan, S., 2019. Stiffness: A new perspective on generalization in neural networks. *arXiv preprint arXiv:1901.09491* .
- [24] Fout, A., Byrd, J., Shariat, B., Ben-Hur, A., 2017. Protein interface prediction using graph convolutional networks. *Advances in neural information processing systems* 30.
- [25] Frenkel, D., Smit, B., 2001. *Understanding molecular simulation: from algorithms to applications*. volume 1. Elsevier.
- [26] Frye, C., de Mijolla, D., Begley, T., Cowton, L., Stanley, M., Feige, I., 2020. Shapley explainability on the data manifold. *arXiv preprint arXiv:2006.01272* .
- [27] Fuchs, F.B., Worrall, D.E., Fischer, V., Welling, M., 2020. Se (3)-transformers: 3d rotation-equivariant attention networks. *arXiv preprint arXiv:2006.10503* .
- [28] Ganea, O.E., Huang, X., Bunne, C., Bian, Y., Barzilay, R., Jaakkola, T., Krause, A., 2021. Independent se (3)-equivariant models for end-to-end rigid protein docking. *arXiv preprint arXiv:2111.07786* .
- [29] Gilmer, J., Schoenholz, S.S., Riley, P.F., Vinyals, O., Dahl, G.E., 2017. Neural message passing for quantum chemistry, in: *International conference on machine learning*, PMLR. pp. 1263–1272.
- [30] Gori, M., Monfardini, G., Scarselli, F., 2005. A new model for learning in graph domains, in: *Proceedings. 2005 IEEE international joint conference on neural networks*, pp. 729–734.
- [31] Greydanus, S., Dzamba, M., Yosinski, J., 2019. Hamiltonian neural networks. *Advances in Neural Information Processing Systems* 32.
- [32] Hamilton, W., Ying, Z., Leskovec, J., 2017. Inductive representation learning on large graphs. *Advances in neural information processing systems* 30.
- [33] Hammer, B., Micheli, A., Sperduti, A., 2005. Universal approximation capability of cascade correlation for structures. *Neural Computation* 17, 1109–1159.
- [34] Hernández, A., Amigó, J.M., 2021. Attention mechanisms and their applications to complex systems. *Entropy* 23, 283.
- [35] Hornik, K., Stinchcombe, M., White, H., 1989. Multilayer feedforward networks are universal approximators. *Neural networks* 2, 359–366.
- [36] Huang, K., Xiao, C., Glass, L.M., Zitnik, M., Sun, J., 2020. Skipggnn: predicting molecular interactions with skip-graph networks. *Scientific reports* 10, 1–16.
- [37] Huang, W., Han, J., Rong, Y., Xu, T., Sun, F., Huang, J., 2022. Equivariant graph mechanics networks with constraints. *arXiv preprint arXiv:2203.06442* .
- [38] Hutchinson, M.J., Le Lan, C., Zaidi, S., Dupont, E., Teh, Y.W., Kim, H., 2021. Lietransformer: Equivariant self-attention for lie groups, in: *International Conference on Machine Learning*, PMLR. pp. 4533–4543.
- [39] Ingraham, J., Garg, V.K., Barzilay, R., Jaakkola, T., 2019. Generative models for graph-based protein design .

- [40] Jin, W., Barzilay, R., Jaakkola, T., 2020. Multi-objective molecule generation using interpretable substructures, in: International conference on machine learning, PMLR. pp. 4849–4859.
- [41] Jumper, J., Evans, R., Pritzel, A., Green, T., Figurnov, M., Ronneberger, O., Tunyasuvunakool, K., Bates, R., Žídek, A., Potapenko, A., Bridgland, A., Meyer, C., Kohl, S.A.A., Ballard, A.J., Cowie, A., Romera-Paredes, B., Nikolov, S., Jain, R., Adler, J., Back, T., Petersen, S., Reiman, D., Clancy, E., Zielinski, M., Steinegger, M., Pacholska, M., Berghammer, T., Bodenstein, S., Silver, D., Vinyals, O., Senior, A.W., Kavukcuoglu, K., Kohli, P., Hassabis, D., 2021. Highly accurate protein structure prediction with AlphaFold. Nature doi:[10.1038/s41586-021-03819-2](https://doi.org/10.1038/s41586-021-03819-2). (Accelerated article preview).
- [42] Karplus, M., McCammon, J.A., 2002. Molecular dynamics simulations of biomolecules. Nature structural biology 9, 646–652.
- [43] Kingma, D.P., Ba, J., 2014. Adam: A method for stochastic optimization. arXiv preprint arXiv:1412.6980 .
- [44] Kipf, T.N., Welling, M., 2016. Semi-supervised classification with graph convolutional networks. arXiv preprint arXiv:1609.02907 .
- [45] Klicpera, J., Becker, F., Günnemann, S., 2021. Gemnet: Universal directional graph neural networks for molecules. arXiv preprint arXiv:2106.08903 .
- [46] Klicpera, J., Bojchevski, A., Günnemann, S., 2018. Predict then propagate: Graph neural networks meet personalized pagerank. arXiv preprint arXiv:1810.05997 .
- [47] Klicpera, J., Giri, S., Margraf, J.T., Günnemann, S., 2020a. Fast and uncertainty-aware directional message passing for non-equilibrium molecules. arXiv preprint arXiv:2011.14115 .
- [48] Klicpera, J., Groß, J., Günnemann, S., 2020b. Directional message passing for molecular graphs. arXiv preprint arXiv:2003.03123 .
- [49] Krizhevsky, A., Hinton, G., et al., 2009. Learning multiple layers of features from tiny images .
- [50] Leman, A., Weisfeiler, B., 1968. A reduction of a graph to a canonical form and an algebra arising during this reduction. Nauchno-Technicheskaya Informatsiya 2, 12–16.
- [51] Li, Q., Han, Z., Wu, X.M., 2018a. Deeper insights into graph convolutional networks for semi-supervised learning, in: Thirty-Second AAAI conference on artificial intelligence.
- [52] Li, Y., Wu, J., Tedrake, R., Tenenbaum, J.B., Torralba, A., 2018b. Learning particle dynamics for manipulating rigid bodies, deformable objects, and fluids. arXiv preprint arXiv:1810.01566 .
- [53] Li, Z., Cui, Z., Wu, S., Zhang, X., Wang, L., 2019. Fi-gnn: Modeling feature interactions via graph neural networks for ctr prediction, in: Proceedings of the 28th ACM International Conference on Information and Knowledge Management, pp. 539–548.
- [54] Liu, Y., Wang, L., Liu, M., Zhang, X., Oztekin, B., Ji, S., 2021. Spherical message passing for 3d graph networks. arXiv preprint arXiv:2102.05013 .
- [55] Liu, Y., Yuan, H., Cai, L., Ji, S., 2020. Deep learning of high-order interactions for protein interface prediction, in: Proceedings of the 26th ACM SIGKDD international conference on knowledge discovery & data mining, pp. 679–687.
- [56] Lu, C., Liu, Q., Wang, C., Huang, Z., Lin, P., He, L., 2019. Molecular property prediction: A multilevel quantum interactions modeling perspective, in: Proceedings of the AAAI Conference on Artificial Intelligence, pp. 1052–1060.
- [57] Maron, H., Ben-Hamu, H., Shamir, N., Lipman, Y., 2018. Invariant and equivariant graph networks. arXiv preprint arXiv:1812.09902 .

- [58] Mrowca, D., Zhuang, C., Wang, E., Haber, N., Fei-Fei, L.F., Tenenbaum, J., Yamins, D.L., 2018. Flexible neural representation for physics prediction. *Advances in neural information processing systems* 31.
- [59] Nair, A., Roy, A., Meinke, K., 2020. Funcgnn: a graph neural network approach to program similarity, in: *Proceedings of the 14th ACM/IEEE International Symposium on Empirical Software Engineering and Measurement (ESEM)*, pp. 1–11.
- [60] Neyshabur, B., Bhojanapalli, S., McAllester, D., Srebro, N., 2017. Exploring generalization in deep learning. *Advances in neural information processing systems* 30.
- [61] Novak, R., Bahri, Y., Abolafia, D.A., Pennington, J., Sohl-Dickstein, J., 2018. Sensitivity and generalization in neural networks: an empirical study. *arXiv preprint arXiv:1802.08760* .
- [62] Paszke, A., Gross, S., Massa, F., Lerer, A., Bradbury, J., Chanan, G., Killeen, T., Lin, Z., Gimelshein, N., Antiga, L., et al., 2019. Pytorch: An imperative style, high-performance deep learning library. *Advances in neural information processing systems* 32, 8026–8037.
- [63] Qi, S., Wang, W., Jia, B., Shen, J., Zhu, S.C., 2018. Learning human-object interactions by graph parsing neural networks, in: *Proceedings of the European Conference on Computer Vision (ECCV)*, pp. 401–417.
- [64] Ramakrishnan, R., Hartmann, M., Tapavicza, E., Von Lilienfeld, O.A., 2015. Electronic spectra from tddft and machine learning in chemical space. *The Journal of chemical physics* 143, 084111.
- [65] Rong, Y., Bian, Y., Xu, T., Xie, W., Wei, Y., Huang, W., Huang, J., 2020. Self-supervised graph transformer on large-scale molecular data. *arXiv preprint arXiv:2007.02835* .
- [66] Rudin, C., 2019. Stop explaining black box machine learning models for high stakes decisions and use interpretable models instead. *Nature Machine Intelligence* 1, 206–215.
- [67] Russakovsky, O., Deng, J., Su, H., Krause, J., Satheesh, S., Ma, S., Huang, Z., Karpathy, A., Khosla, A., Bernstein, M., et al., 2015. Imagenet large scale visual recognition challenge. *International journal of computer vision* 115, 211–252.
- [68] Sanchez-Gonzalez, A., Godwin, J., Pfaff, T., Ying, R., Leskovec, J., Battaglia, P., 2020. Learning to simulate complex physics with graph networks, in: *International Conference on Machine Learning, PMLR*. pp. 8459–8468.
- [69] Sanchez-Gonzalez, A., Heess, N., Springenberg, J.T., Merel, J., Riedmiller, M., Hadsell, R., Battaglia, P., 2018. Graph networks as learnable physics engines for inference and control, in: *International Conference on Machine Learning, PMLR*. pp. 4470–4479.
- [70] Satorras, V.G., Hoogeboom, E., Welling, M., 2021. E (n) equivariant graph neural networks, in: *International Conference on Machine Learning, PMLR*. pp. 9323–9332.
- [71] Scarselli, F., Gori, M., Tsoi, A.C., Hagenbuchner, M., Monfardini, G., 2008a. Computational capabilities of graph neural networks. *IEEE Transactions on Neural Networks* 20, 81–102.
- [72] Scarselli, F., Gori, M., Tsoi, A.C., Hagenbuchner, M., Monfardini, G., 2008b. The graph neural network model. *IEEE transactions on neural networks* 20, 61–80.
- [73] Schütt, K.T., Arbabzadah, F., Chmiela, S., Müller, K.R., Tkatchenko, A., 2017. Quantum-chemical insights from deep tensor neural networks. *Nature communications* 8, 1–8.
- [74] Schütt, K.T., Sauceda, H.E., Kindermans, P.J., Tkatchenko, A., Müller, K.R., 2018. SchNet—a deep learning architecture for molecules and materials. *The Journal of Chemical Physics* 148, 241722.
- [75] Senior, A.W., Evans, R., Jumper, J., Kirkpatrick, J., Sifre, L., Green, T., Qin, C., Žídek, A., Nelson, A.W., Bridgland, A., et al., 2020. Improved protein structure prediction using potentials from deep learning. *Nature* 577, 706–710.

- [76] Shwartz-Ziv, R., Tishby, N., 2017. Opening the black box of deep neural networks via information. arXiv preprint arXiv:1703.00810 .
- [77] Stärk, H., Ganea, O.E., Pattanaik, L., Barzilay, R., Jaakkola, T., 2022. Equibind: Geometric deep learning for drug binding structure prediction. arXiv preprint arXiv:2202.05146 .
- [78] Thomas, N., Smidt, T., Kearnes, S., Yang, L., Li, L., Kohlhoff, K., Riley, P., 2018. Tensor field networks: Rotation-and translation-equivariant neural networks for 3d point clouds. arXiv preprint arXiv:1802.08219 .
- [79] Tolstikhin, I., Houlsby, N., Kolesnikov, A., Beyer, L., Zhai, X., Unterthiner, T., Yung, J., Steiner, A.P., Keysers, D., Uszkoreit, J., Lucic, M., Dosovitskiy, A., 2021. Mlp-mixer: An all-mlp architecture for vision, in: Advances in Neural Information Processing Systems (NIPS).
- [80] Topping, J., Di Giovanni, F., Chamberlain, B.P., Dong, X., Bronstein, M.M., 2021. Understanding over-squashing and bottlenecks on graphs via curvature. arXiv preprint arXiv:2111.14522 .
- [81] Tsang, M., Cheng, D., Liu, Y., 2017. Detecting statistical interactions from neural network weights. arXiv preprint arXiv:1705.04977 .
- [82] Tuckerman, M., 2010. Statistical mechanics: theory and molecular simulation. Oxford university press.
- [83] Vaswani, A., Shazeer, N., Parmar, N., Uszkoreit, J., Jones, L., Gomez, A.N., Kaiser, Ł., Polosukhin, I., 2017. Attention is all you need. Advances in neural information processing systems 30.
- [84] Veličković, P., Cucurull, G., Casanova, A., Romero, A., Lio, P., Bengio, Y., 2017. Graph attention networks. arXiv preprint arXiv:1710.10903 .
- [85] Virtanen, P., Gommers, R., Oliphant, T.E., Haberland, M., Reddy, T., Cournapeau, D., Burovski, E., Peterson, P., Weckesser, W., Bright, J., et al., 2020. Scipy 1.0: fundamental algorithms for scientific computing in python. Nature methods 17, 261–272.
- [86] Wang, X., Wu, Y., Zhang, A., He, X., Chua, T.S., 2021. Towards multi-grained explainability for graph neural networks. Advances in Neural Information Processing Systems 34.
- [87] Wang, X., Zhang, A., Hu, X., Feng, F., He, X., Chua, T.S., et al., 2022. Deconfounding to explanation evaluation in graph neural networks. arXiv preprint arXiv:2201.08802 .
- [88] Weng, T.W., Zhang, H., Chen, P.Y., Yi, J., Su, D., Gao, Y., Hsieh, C.J., Daniel, L., 2018. Evaluating the robustness of neural networks: An extreme value theory approach. arXiv preprint arXiv:1801.10578 .
- [89] Whiteside, D.T., 1966. Newtonian dynamics. History of Science 5, 104.
- [90] Wieder, O., Kohlbacher, S., Kuenemann, M., Garon, A., Ducrot, P., Seidel, T., Langer, T., 2020. A compact review of molecular property prediction with graph neural networks. Drug Discovery Today: Technologies 37, 1–12.
- [91] Wu, F., Zhang, Q., Radev, D., Cui, J., Zhang, W., Xing, H., Zhang, N., Chen, H., 2021. 3d-transformer: Molecular representation with transformer in 3d space. arXiv preprint arXiv:2110.01191 .
- [92] Wu, Y.X., Wang, X., Zhang, A., He, X., Chua, T.S., 2022. Discovering invariant rationales for graph neural networks. arXiv preprint arXiv:2201.12872 .
- [93] Wu, Z., Pan, S., Chen, F., Long, G., Zhang, C., Philip, S.Y., 2020. A comprehensive survey on graph neural networks. IEEE transactions on neural networks and learning systems 32, 4–24.
- [94] Wu, Z., Ramsundar, B., Feinberg, E.N., Gomes, J., Geniesse, C., Pappu, A.S., Leswing, K., Pande, V., 2018. Moleculenet: a benchmark for molecular machine learning. Chemical science 9, 513–530.

- [95] Xie, T., Grossman, J.C., 2018. Crystal graph convolutional neural networks for an accurate and interpretable prediction of material properties. *Physical review letters* 120, 145301.
- [96] Xiong, Z., Wang, D., Liu, X., Zhong, F., Wan, X., Li, X., Li, Z., Luo, X., Chen, K., Jiang, H., et al., 2019. Pushing the boundaries of molecular representation for drug discovery with the graph attention mechanism. *Journal of medicinal chemistry* 63, 8749–8760.
- [97] Xu, K., Hu, W., Leskovec, J., Jegelka, S., 2018. How powerful are graph neural networks? *arXiv preprint arXiv:1810.00826* .
- [98] Yang, K., Swanson, K., Jin, W., Coley, C., Eiden, P., Gao, H., Guzman-Perez, A., Hopper, T., Kelley, B., Mathea, M., et al., 2019. Analyzing learned molecular representations for property prediction. *Journal of chemical information and modeling* 59, 3370–3388.
- [99] Yu, J., Xu, T., Rong, Y., Bian, Y., Huang, J., He, R., 2020. Graph information bottleneck for subgraph recognition. *arXiv preprint arXiv:2010.05563* .
- [100] Zhang, H., Li, S., Ma, Y., Li, M., Xie, Y., Zhang, Q., 2020a. Interpreting and boosting dropout from a game-theoretic view. *arXiv preprint arXiv:2009.11729* .
- [101] Zhang, S., Liu, Y., Xie, L., 2020b. Molecular mechanics-driven graph neural network with multiplex graph for molecular structures. *arXiv preprint arXiv:2011.07457* .
- [102] Zügner, D., Akbarnejad, A., Günnemann, S., 2018. Adversarial attacks on neural networks for graph data, in: *Proceedings of the 24th ACM SIGKDD International Conference on Knowledge Discovery & Data Mining*, pp. 2847–2856.

A Theoretical Analysis

A.1 Proof of Multi-order Interactions

There we explain why $I^{(m)}(i, j)$ has no difference whether we include variables $\{i, j\}$ in S or not. In the setting of [100, 18], $I^{(m)}(i, j)$ takes the following form:

$$I^{(m)}(i, j) = \mathbb{E}_{S \subseteq N \setminus \{i, j\}, |S|=m} [\Delta f(i, j, S)], \quad (5)$$

where $\Delta f(i, j, S) = f(S \cup \{i, j\}) - f(S \cup \{i\}) - f(S \cup \{j\}) + f(S)$ and $i, j \notin S$. While in our formulation, the order $m' = m + 2$ corresponds to the context $S' = S \cup \{i, j\}$. Now we denote our version of the multi-order interaction as $I^{(m')}(i, j)$ with $\Delta' f(i, j, S)$ and aim to show that $I^{(m)}(i, j) = I^{(m')}(i, j)$.

It is trivial to obtain that $f(S \cup \{i, j\}) - f(S \cup \{i\}) - f(S \cup \{j\}) + f(S) = f(S') - f(S' \setminus \{i\}) - f(S' \setminus \{j\}) + f(S' \setminus \{i, j\})$, which indicates that $\Delta f(i, j, S) = \Delta' f(i, j, S')$. Therefore, we can get $I^{(m+2)}(i, j) = I^{(m')}(i, j)$.

A.2 Theoretical Distributions of $F^{(m)}$

Fig. 9 depicts the theoretical distributions of $F^{(m)}$ for different n . Unlike Fig. 1, the empty set \emptyset is allowed as the input for DNNs. Apparently, when the number of variables n is very large ($n \geq 100$), $F^{(m)}$ is only positive for $\frac{m}{n} \rightarrow 0$. For macromolecules such as proteins, the number of atoms are usually more than ten thousands. If the theorem in [18] that the strengths $\Delta W^{(m)}(i, j)$ of learning the m -order interaction is strictly proportional to $F^{(m)}$ holds, DNNs would be impossible to put attention to any middle-order interactions, which is proven to be critical for modeling protein-protein interactions [55, 17].

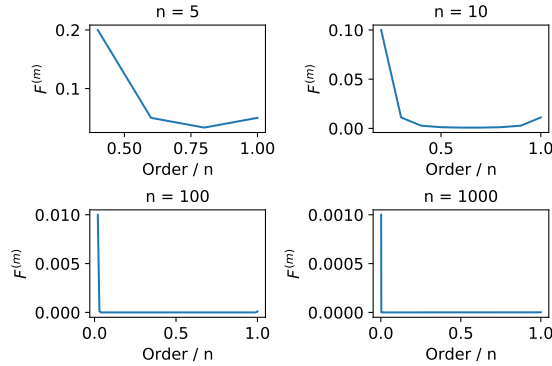


Figure 9: Distributions of $F^{(m)}$ with different numbers of variables n where $f(\emptyset)$ is taken into consideration.

A.3 Explanation of Proposition 1

Prop. 1 illustrates an intuitive necessary condition for a model f to achieve the global minimum loss. That is, the learned strength $J^{(m)}$ must match the optimal strength $J^{(m)*}$. Otherwise, f must be inferior to the best predictor f^* . This proposition is very straightforward. The global minimum loss L^* has its corresponding model weight f^* and thereby a unique learned strength $J^{(m)*}$. Given another model f , if its strength $J^{(m)}$ is different from $J^{(m)*}$, then f is different from f^* . As a consequence, the loss of f must be larger than L^* . Notably, there we consider the loss function to be non-convex. In contrast, if the loss function is convex, standard optimization techniques like gradient descent will easily find parameters that converge towards global minima.

B Re-implementation of CNNs on Visual Tasks

We re-run the official code provided by Deng et al. [18] and investigate the change of interaction strengths during the training process. Fig. 2 plots the corresponding strengths at different epochs, where the dotted line denotes the initial interaction strength without training, i.e., the data distribution of strengths $J_D^{(m)}$. It can be easily found that $J_D^{(m)}$ in both CIFAR-10 and ImageNet have already obeyed a mode that the low-order ($\frac{m}{n} \leq 0.2$) and high-order ($\frac{m}{n} \geq 0.8$) interaction strengths are much higher than middle-order ($0.2 \leq \frac{m}{n} \leq 0.8$). The variation of interaction strengths is very slight with the training proceeding, which validates our statement that the data distribution has a strong impact on the learned distribution. More importantly, we challenge the argument in Deng et al. [18], who believe it is difficult for DNNs to encode middle-order interaction. But in our experiments on GNNs, we document that DL-based models are capable of capturing middle-order interactions.

C Experimental Details and Additional Results

C.1 Newtonian Dynamics Dataset

The following six forces are utilized in the dataset of Newtonian dynamics: (1) $1/r$ orbital force: $-m_1 m_2 \hat{r}/r$; (2) $1/r^2$ orbital force $-m_1 m_2 \hat{r}/r^2$; (3) charged particles force $q_1 q_2 \hat{r}/r^2$ (4) damped springs with $|r - 1|^2$ potential and damping proportional and opposite to speed; (5) discontinuous forces, $-\{0, r^2\} \hat{r}$, switching to 0 force for $r < 2$; and (6) springs between all particles, a $(r - 1)^2$ potential. There we only use the spring force for our experiments.

C.2 Training Details

All experiments are implemented by Pytorch [62] on an A-100 GPU. An Adam [43] optimizer is used without weight decay, and a ReduceLROnPlateau scheduler is enforced to adjust it with a factor of 0.6 and a patience of 10. The initial learning rate is $1e-4$, and the minimum learning rate is $5e-6$. The batch size is 512 for the sake of a fast training speed. Each model is trained for 1200 epochs, and an early stopping is used if the validation error fails to decrease for 30 successive epochs. We randomly split each dataset into training, validation, and test sets with a ratio of 80/10/10. For both EGNN and Molformer, the numbers of layers (i.e., depths) are 3, and the dimensions of the input feature are 32. Besides, Molformer has 4 attention heads and a dropout rate of 0.1. Its dimension of the feed-forward network is 128. It is worth noting that we employ the multi-scale self-attention with a distance bar of $[0.8, 1.6, 3]$ to achieve better performance. This multi-scale mechanism helps Molformer to concentrate more on local contexts. However, it does no harm to FC-graphs, and the connections between all pairs of entities remain. We also discover that the multi-scale mechanism has little impact on the distribution of $J^{(m)}$ and $J_D^{(m)}$. Regarding the setup of the ISGR algorithm, the threshold \bar{J} to adjust the number of neighbors is tuned via a grid search. The interval of epochs is 10, and the initial $k_0 = 8$.

We create a simulated system with 10 identical particles with a unit weight for Hamiltonian and Newtonian cases. For QM7, QM8, and ISO17 datasets, we sample 10 molecules that have the lowest MAE. For Hamiltonian and Newtonian datasets, we sample 10 timeframes that have the lowest prediction errors. Then for each molecule or dynamic system, we compute all pairs of entities $i, j \in [N]$ without any sampling strategy. Moreover, we limit the number of atoms between 10 and 18 to compute the interaction strengths for QM7 and MQ8.

C.3 Examination of the Normal Distribution Hypothesis

We use *scipy.stats.normaltest* in the Scipy package [85] to test the null hypothesis that $\frac{\partial \Delta f(i,j,S)}{\partial W}$ comes from a normal distribution, i.e., $\frac{\partial \Delta f(i,j,S)}{\partial W} \sim \mathcal{N}(0, \sigma^2)$. This test is based on D’Agostino and Pearson’s examination that combines skew and kurtosis to produce an omnibus test of normality. The p -values of well-trained EGNN and Molformer on the Hamiltonian dynamics dataset are $1.97147e-11$ and $2.38755e-10$, respectively. The p -values of randomly initialized EGNN and Molformer on the Hamiltonian dynamics dataset are $2.41749e-12$ and $9.78953e-07$, separately. Therefore, we are highly confident to reject the null hypothesis (e.g., $\alpha = 0.01$) and insist that $\frac{\partial \Delta f(i,j,S)}{\partial W}$ depends on the data distributions of downstream tasks and the backbone model architectures.

C.4 Distributions of Strengths in QM7

Due to the limitation of space, we move Fig. 10 to Appendix, which shows the learned distribution and data distribution of EGNN and Molformer in the QM7 dataset. The conclusions are very similar to the discovery in QM8. Although the data distribution of strengths $J_D^{(m)}$ concentrate on low-order ($\frac{m}{n} \leq 0.4$), the learned distribution of strengths $J^{(m)}$ are mainly allocated on middle-order interactions ($0.5 \leq \frac{m}{n} \leq 0.7$). Especially for EGNN, its spike of $J^{(m)}$ is at $m = 9$. While concerning Molformer, the segment of its $J^{(m)}$ that increases most is dispersive between $0.3 \leq \frac{m}{n} \leq 0.5$.

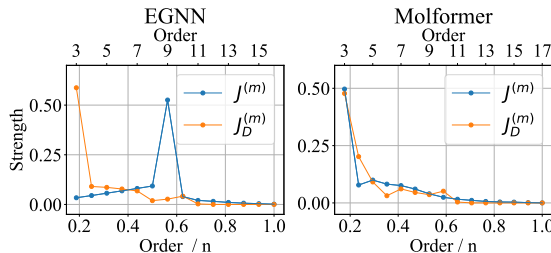


Figure 10: Learned and data distributions of the interaction strength of EGNN and Molformer in the QM7 dataset.

D More Related Work on Representation Capability of GNNs

It is well-known that MLP can approximate any Borel measurable function [35], but few study the universal approximation capability of GNNs [93]. Hammer et al. [33] demonstrates that cascade correlation can approximate functions with structured outputs. Scarselli et al. [71] prove that a RecGNN [72] can approximate any function that preserves unfolding equivalence up to any degree of precision. Maron et al. [57] show that an invariant GNN can approximate an arbitrary invariant function defined on graphs. Xu et al. [97] show that common GNNs including GCN [44] and GraphSage [32] are incapable of differentiating different graph structures. They further prove if the aggregation functions and the readout functions of a GNN are injective, it is at most as powerful as the Weisfieler-Lehman (WL) test [50] in distinguishing different graphs.

E Can motif-based heterogeneous graphs address the bottleneck?

Recently, there has been an appealing trend to decouple the input graph from the initial graph for better information propagation. Most are explained from alleviating the *over-squashing* problem [1]. There we offer another explanation from the perspective of optimizing the inductive bias of GNNs. Recall that, Wu et al. [91] regard motifs (e.g., functional groups) as independent nodes and combine them with atom-level nodes to formulate heterogeneous molecular graphs (HMGs). The goal of HMGs is to assist models in learning better representations of those motif-based subgraphs, namely, to simultaneously promote GNNs’ attention on middle-order interactions. Nonetheless, HMGs require external domain knowledge, which can be difficult to obtain. Inversely, our ISGR method is entirely data-driven and more suitable for tasks that lack chemical or physical domain knowledge.